SLAC-PUB-65
December 1964

PHOTOPRODUCTION OF NEUTRAL K-MESONS*

S. D. Drell and M. Jacob†
Stanford Linear Accelerator Center, Stanford University, Stanford, California

ABSTRACT

Photoproduction of a neutral K-meson beam at high energies from hydrogen is computed in terms of a K^* vector meson exchange mechanism corrected for final state interactions. The results are very encouraging for the intensity of high energy K_2 beams at high energy electron accelerators. A typical magnitude is 20 μb/ster for a lower limit of the K_o photoproduction differential cross section, at a laboratory peak angle of 2°, for 15 BeV incident photons.

(Submitted to the Physical Review)

---

*Work supported in part by U.S. Atomic Energy Commission.

†On leave of absence from Service de Physique Theorique, Saclay, Gif-sur-Yvette, France.

INTRODUCTION

We compute the cross section for photoproduction of K^o mesons at high energies

$$\gamma + p \rightarrow K^o + \Sigma^+ \qquad (1)$$

due to the mechanism illustrated in Fig. 1, i.e., via K^* exchange. Our purpose is to obtain an estimate for the neutral K beam which may be produced with high energy electron machines. There is now experimental evidence that vector meson exchange plays an important role in high energy two-body or quasi two-body reactions.[1] Furthermore, in reaction (1) the K^* meson is the lightest particle with the quantum numbers of the t channel, since there is no K^o current. We thus expect K^* exchange to be a dominant feature in high energy K^o photoproduction.

Nevertheless, one should not be satisfied with a simple Born approximation calculation as illustrated by Fig. 1. In order to reproduce experimental data in the 2 to 4 BeV range, the one-meson-exchange approximation has to be corrected to take proper care of the existence of many competing channels. This correction has been applied with great success by Gottfried and Jackson[2] and other authors to several reactions. The method used is the distorted wave Born approximation, currently applied in low energy nuclear physics. Each

partial wave amplitude F_j is obtained from the Born approximation partial wave contribution B_j, through the following relation:

$$F_j(s) = e^{i\delta_{jf}(s)} B_j(s) e^{i\delta_{ji}(s)} \tag{2}$$

where δ_{jf} and δ_{ji} are the scattering phase shifts (generally complex) for angular momentum j in the final and initial states; s stands for the CM energy squared. This method provides an answer free of adjustable parameters when the elastic scattering amplitudes for the initial and final two-body systems are purely imaginary. The inelasticity parameters $\eta_j = \left| e^{2i\delta_j} \right|$ can then be obtained from the shape of the elastic diffraction peak and the total cross section.

It must be pointed out though that this distorted wave approximation, as expressed by (2), does not in general have a firm theoretical basis in application to high energy reactions. Where it is valid, as has been recently shown by Omnès[3], is for partial waves with inelasticity parameters that are not too different from unity. Nevertheless, if (2) is not formally correct for low partial waves, where the absorption is large, it does give the correct qualitative behavior of a strong damping of the two-body reaction amplitude due to the effect of many open competing channels. In other words, we expect the statistical model to be more reliable than the one meson exchange approximation when calculating the low partial wave amplitudes. Since there are so many open channels, these particular two-body channels of low angular momentum should enter with a small amplitude and

not play a dominant role in the total amplitude.

We do not expect then that (2), used for all partial waves, will give a result much different from what could be obtained with a more refined procedure, and it should be adequate in order to yield an estimate of the cross section. In particular we present results corresponding to the maximum possible absorption (no S wave at all) in this formalism in order to make a pessimistic estimate of the K^{o} beam intensity.

This treatment protects unitarity in the incident and outgoing channels by including the possibility of transition to all the open inelastic channels, as first discussed by Sopkovitch and Baker and Blankenbecler.[4] Its main effect is to reduce the Born approximation predictions and to make the angular distribution more strongly peaked at small angles.

In the photoproduction process, the corrections come only from the strong final state interactions. Equation (2) is then replaced by ($\eta_{ji} \approx 1$)

$$F_j(s) = \sqrt{\eta_j(s)}B_j(s) \quad . \tag{3}$$

To obtain the photoproduction cross section for K^{o} mesons we must still insert values for the $K^{*}K^{o}\gamma$ coupling constant, or the K^{o*} radiative decay width, as well as for the $K^{*}p\Sigma$ coupling constant in the B_j amplitudes, and for the $K\Sigma$ elastic scattering angular distribution and total cross section for the absorption factor η_j. In order to obtain a reliable order of magnitude we

may with some confidence use SU_3 symmetry to relate these parameters to already known quantities. We can, in this way, make predictions for the K^o photoproduction cross section in terms of "experimental" parameters.

Our calculation follows the same lines as one already carried out for the $p\bar{p} \rightarrow \Lambda\bar{\Lambda}$ reaction in the 3-4 BeV/c range. In this process K^* exchange[5] dominates, as shown in Fig. 2, but with the low partial waves absorbed out using the model of Gottfried and Jackson. An extremely good fit to the experimental data is obtained assuming identical inelasticity parameters for the $p\bar{p}$ and $\Lambda\bar{\Lambda}$ channels and a $K^*p\Lambda$ coupling constant obtained from the ρ nucleon coupling constant by SU_3 symmetry.

Although this strengthens our confidence in the model, one must be aware of the fact that we want to obtain a cross section estimate for (1) at energies ranging from 10 to 20 BeV, which are much higher than the energy range in which it has proved successful (2-4 BeV). In using this approximation we assume that the vector meson exchange contribution remains the dominant feature when the energy increases.

Our motivation in carrying out this calculation, is to emphasize the strong suggestion that an intense "healthy" K_2 beam will emerge from high energy electron accelerators (SLAC in particular) and will be available for detailed experimental studies.

In the spirit of making such an experimental prediction we shall bias the calculations in the following section so as to yield a lower

limit prediction by overemphasizing absorption from the final $K^{o}\Sigma^{+}$ channel. The final results are shown graphically in Figs. 3, 4, 5, and 6 illustrate the reduction from the simple one particle exchange amplitude when absorption is taken into account in the individual partial waves.

CALCULATIONS

In the simple one particle exchange approximation the amplitude for Fig. 1 with the indicated kinematics is written

$$\mathcal{M} = g_{K^*K\gamma} \frac{g_{K^*p\Sigma}}{m^*} \sqrt{\frac{M_N M_\Sigma}{4k\omega E_1 E_2}} (2\pi)^4 \delta^4 (q+p_2-p_1-k) F \tag{4}$$

where

$$F \equiv \frac{\epsilon_{\mu\nu\sigma\tau} \epsilon^{\mu} k^{\nu} q^{\sigma} \left\{ \bar{u}(p_2) \gamma^{\tau} u(p_1) \right\}}{(q-k)^2 - m^{*2}} \tag{5}$$

ϵ is the photon polarization vector, m^* denotes the K^* mass, and M_N and M_Σ the nucleon and Σ mass respectively. The $K^*K\gamma$ vertex with the coupling constant $g_{K^*K\gamma}$ has the unique form shown by the antisymmetric outer product in the numerator of (5), up to a form factor depending on momentum transfer $t = (q-k)^2$. This form factor dependence on t is neglected here, since in the region of interest at the peak of the differential cross section $|t| < m^{*2}$. The relation of $g_{K^*K\gamma}$ to the radiative decay width $\Gamma_{K^* \to K\gamma}$ is given by

$$\frac{g^2_{K^*K\gamma}}{4\pi} = \frac{24\Gamma_{K^* \to K\gamma}}{m^*(1-m^2/m^{*2})^{3/2}} \tag{6}$$

where m stands for the K mass. The coupling strength at the $K^*p\Sigma$ vertex $g_{K^*p\Sigma}\bar{u}(p_2)\gamma_\mu u(p_1)$ is denoted by $g_{K^*p\Sigma}$. A Pauli type coupling is neglected as relatively unimportant for low momentum transfers.

The differential cross section in the center-of-mass system for unpolarized particles is given by

$$\left(\frac{d\sigma}{d\Omega}\right)_{cm} = \frac{q}{k}\frac{M_N M_\Sigma}{W^2 m^{*2}}\left(\frac{g^2_{K^*K\gamma}}{4\pi}\right)\left(\frac{g^2_{K^*p\Sigma}}{4\pi}\right)\frac{1}{2}\sum_{\text{Pol}}\frac{1}{2}\sum_{\text{Spin}}|F|^2 \tag{7}$$

where W denotes the total energy.

Direct calculation of (4), (5) and (7) gives an upper limit in the absence of final state interaction and we quote the result here in order to provide a general orientation. In the laboratory system and in the limit of small angles and high energies, we find

$$\left(\frac{d\sigma}{d\Omega}\right)_{\substack{\text{lab}\\ M/k \to 0\\ \theta \to 0}} = \frac{1}{2m^{*2}}\left(\frac{g^2_{K^*p\Sigma}}{4\pi}\right)\left(\frac{g^2_{K^*K\gamma}}{4\pi}\right)\frac{\theta^2_{\text{lab}}}{\left[\theta^2_{\text{lab}} + m^{*2}/k^2_{\text{lab}}\right]^2} \tag{8}$$

Putting $\frac{g^2_{K^*p\Sigma}}{4\pi} \sim 1$ and $\frac{g^2_{K^*K\gamma}}{4\pi} \sim \frac{1}{137}$, as becomes an electromagnetic

transition corresponding to a radiative decay width ~ 0.1 MeV in (6), we find at the peak angle $\theta_{lab} = m^*/k_{lab}$ and at an incident photon energy of $k_L = 15$ BeV,

$$\left(\frac{d\sigma}{d\Omega}\right)_{peak} \approx 100 \frac{\mu b}{ster} . \qquad (9)$$

We can compute with this production cross section the K_2 yield with an incident beam intensity of 20 BeV electrons of 10^{14}/sec. as predicted for SLAC. Through a 1/10 radiation length target there will emerge $10^{13} \frac{dk}{k}$ photons per second in an energy interval dk about k, or 6×10^{11} photons per BeV-sec. at 15 BeV. If these photons are incident on a 2 gram/cm^2 hydrogen target the resulting long-lived K_2 flux is 5×10^5/sec. within a solid angle of $\pi \frac{m^{*2}}{k^2} \approx 10^{-2}$ ster about $\theta = m^*/k \approx 3°$.

In analyzing the effect of final state interactions it has been found to be necessary to treat the particle spins correctly in order to avoid unphysical diffraction bumps in the calculated angular distributions. Since our primary interest here is in the formation of a secondary beam of K_2's of high flux and in view of uncertainties in the coupling constants $g_{K^*\Sigma p}$ and $g_{\gamma K^* K}$, it suffices to make a simple spinless impact parameter calculation of the absorption from the $K^o\Sigma^+$ channel. The qualitative results obtained in this way are then confirmed by a detailed calculation performed by decomposing the amplitude F into individual helicity and angular momentum channels and then absorbing each partial wave with the parameters computed from the diffraction scattering.

First we present the simple result. The peak in the differential cross section (8) occurs at the angle $\theta = m^*/k$ corresponding to a

momentum transfer $k\theta = \sqrt{|t|} = m^*$. This defines an impact parameter $b = 1/m^*$ and according to the distorted wave Born approximation the final state amplitude is diminished by the factor

$$\sqrt{\eta(b)} = \left\{ 1 - \frac{\sigma_t(s)}{4\pi A(s)} e^{-b^2/2A(s)} \right\}^{\frac{1}{2}} \tag{10}$$

representing the fractional absorption of the $K^O\Sigma^+$ system into other channels when they collide with impact parameter b. In (10), σ_t is the $K^O\Sigma^+$ collision cross section at energy $\sqrt{s}$, and the approximation is made that the amplitude for $K^O\Sigma^+$ scattering is imaginary, i.e.,

$$f(s,0) = \mathrm{Im}f(s,0) = \frac{k}{4\pi} \sigma_t(s) .$$

and that for small finite momentum transfer, the amplitude is parameterized as

$$f(s,t) = e^{-\frac{1}{2}At} f(s,0) \tag{11}$$

A as well as σ_t are fit to π-nucleon high energy scattering parameters. Using 15 BeV data, so that[6]

$$\sigma_t = 27 \text{ mb and } A = 10/(\text{BeV})^2 \tag{12}$$

we evaluate from (10) for $b = 1/m^*$,

$$\sqrt{\eta}\ (b = 1/m^*) = 0.7$$

In terms of their partial wave expansions the individual amplitudes are given by

$$
\begin{aligned}
F_1 &= \sum_{j=1}^{\infty} (j + \tfrac{1}{2}) F_1^j d^j_{\frac{1}{2}-\frac{1}{2}}(\theta) \sqrt{\eta_j} \\
F_2 &= \sum_{j=1}^{\infty} (j + \tfrac{1}{2}) F_2^j d^j_{\frac{3}{2}-\frac{1}{2}}(\theta) \sqrt{\eta_j} \\
F_3 &= \sum_{j=1}^{\infty} (j + \tfrac{1}{2}) F_3^j d^j_{\frac{3}{2}-\frac{1}{2}}(\theta) \sqrt{\eta_j} \\
F_4 &= \sum_{j=1}^{\infty} (j + \tfrac{1}{2}) F_4^j d^j_{-\frac{1}{2}-\frac{1}{2}}(\theta) \sqrt{\eta_j}
\end{aligned}
\tag{17}
$$

where the factor $\sqrt{\eta_j}$ corrects the j-th partial wave channel for the absorption from the final $K^o\Sigma^+$ state. The absorption factor for the j-th partial wave is obtained by substituting for the impact parameter by the classical wave prescription

$$
b \to \frac{\ell}{q} = \frac{j - \frac{1}{2}}{q} \; ; \; \eta_j = \left(1 - \frac{\sigma_t}{4\pi A} e^{-(j-\frac{1}{2})^2/2Aq^2}\right) \tag{18}
$$

Since many partial waves contribute at the high energies of interest little error is introduced by starting the summation at $j - \frac{1}{2} = \frac{1}{2}$ in (14). We also neglect spin-dependence in the absorption.

We have inserted (17) into (18) and added up the contributions for each j. The results are presented in Figs. 3, 4, and 5 for two different energies 10 and 15 BeV photon and at 15 BeV in both the center-of-mass and laboratory systems. Shown in these figures are the Born approximation results given in the high energy and small angle limit

by (8), together with the curves showing successive reduction of the individual partial waves. Moreover since we are interested in a lower bound in the production process in computing the secondary K_2 beam intensities we choose $\sigma_t/4\pi A = 1$ corresponding to maximum S-wave absorption. In Fig. 6 the actual parameters of (9) were used in evaluating (15).

The coupling constants used have been obtained in the following way: SU_3 symmetry[8] relates the $K^*p\Sigma$ and ρ nucleon coupling constants; namely

$$g_{K^*N\Sigma} = \frac{\sqrt{6}}{2} g_{\rho NN} \tag{19}$$

If the ρ meson is assumed to be coupled to the isotopic spin current one further has $g_{\rho NN} = g_{\rho\pi\pi}$. With a ρ meson width of the order of 100 MeV, one infers

$$\frac{g^2_{K^*p\Sigma}}{4\pi} \approx 0.75 \tag{20}$$

The $K^*K\gamma$ and $\rho\pi\gamma$ coupling constants may be easily related by SU_3 symmetry if the electromagnetic current transforms like a member of an octet. This gives $g_{K^*K\gamma} \approx -2g_{\rho\pi\gamma}$. The $\rho\pi\gamma$ coupling constant is then related to the ρ radiative decay width by (6) when the K^* and K masses are respectively replaced by the ρ and π masses. If Γ_γ stands for the ρ radiative decay width, in MeV, we have

$$\frac{g^2_{K^*K\gamma}}{4\pi} \approx 0.13\ \Gamma_\gamma \tag{21}$$

The curves of Figs. 3, 4, 5, and 6 correspond to (20) and (21) with a ρ meson radiative width of 0.15 MeV.

This is a very conservative estimate as recently reported measurements[9] of ρ^o photoproduction, if interpreted as due entirely to one pion exchange, lead to a ρ radiative width of 1.5 MeV, ~ ten times larger. Our results in Figs. 3, 4, and 5 can be scaled simply by the ratio of the observed ρ radiative decay width to the assumed value of 0.15 MeV when data are available.

CONCLUSIONS

Before anyone is tempted to ascribe too much weight to the detailed numerical results we call attention to the fact that a representation of the diffraction scattering of a meson-baryon system by a purely imaginary amplitude, as done in (11), fails to reproduce the recently reported real part of the forward scattering amplitude.[10] Also there is considerable latitude at present in our knowledge of the coupling constants $g_{K^*K\gamma}$ and $g_{K^*p\Sigma}$. The relatively large cross section, obtained from K^* exchange, is due to the fact that absorption, although strong, is mainly confined to the low partial waves ($j < 8$ at 15 BeV). An additional and non-interfering mechanism for photoproducing K^o mesons is via the charged K^* current followed by the subsequent decay $K^{+*} \rightarrow K^o + \pi^+$. As discussed in reference 9 this could be important at small angles if the charged K^* has a non-vanishing anomalous magnetic moment.

These results have to be compared to photoproduction of charged K meson expected at the same energy. Assuming the electromagnetic current to transform like a member of an octet we use charge independence to

obtain a ratio of 1/2 between the $\gamma + p \rightarrow K^+\Sigma^o$, Λ^o and $\gamma + p \rightarrow K^o\Sigma^\pm$ cross sections as computed above. We expect then a K^+ differential cross section of the order of 10 μb/ster at the laboratory peak angle for an incident photon of 15 BeV due to K^* exchange. This is to be compared with a peak differential cross section of $\approx$ 100 μb/ster expected from the K^+ current contribution which is illustrated on Fig. 7, when we include all inelastic final states that can be excited by the normalized equivalent quantum spectrum from an incident 20 BeV electron.

The numerical calculations were carried out on the Stanford B5000 computer. Results as plotted directly by the machine are shown in Fig. 3. It is a pleasure to thank S. Howry for an introduction to the Algol system.

REFERENCES

1. J. D. Jackson, (to be published) Rev. Mod. Phys.
2. K. Gottfried and J. D. Jackson, CERN preprints (1964);
   A. Dar and W. Tobocman, Phys. Rev. Letters 12, 511 (1964);
   L. Durand and Y. T. Chin, Phys. Rev. Letters 12, 339 (1964);
   M. H. Ross and G. L. Shaw, Phys. Rev. Letters 12, 627 (1964).
3. R. Omnès, UCRL preprint, 1964.
4. N. T. Sopkovitch, Nuovo Cimento 26, 186 (1962);
   M. Baker and R. Blankenbecler, Phys. Rev. 128, 415 (1962).
5. G. Cohen and H. Navelet, Saclay preprint (1964).
6. K. J. Foley et al., Phys. Rev. Letters 11, 425 (1963);
   S. Brandt et al., Phys. Rev. Letters 10, 413 (1963).
7. M. Jacob and G. C. Wick, Ann. Phys. (N.Y.) 7, 404 (1959).
8. M. Gell-Mann, California Institute of Technology Report CTSL 20 (1961).
9. H. R. Crouch, Jr., et al., Phys. Rev. Letters 13, 640 (1964). The ρ radiative width would be further increased if the one pion exchange calculations to which the experiments are compared [S. M. Berman and S. D. Drell, Phys. Rev. 133, B791 (1964)] are reduced by the analogous final state corrections as discussed in this paper.
10. S. J. Lindenbaum Rapporteur's talk 1964 International Conference on high energy physics, Dubna.

FIGURE CAPTIONS

1. K^* exchange in photoproduction.
2. K^* exchange in $p\bar{p}$ collision.
3. Center-of-mass differential cross section at 10 BeV. Curve (1) gives the Born approximation. Curve (2) is obtained after subtraction of the $j = \frac{1}{2}$ partial wave. Curves (3) and (4) are respectively obtained after the $j = 1/2, 3/2, 5/2, 7/2$ and all partial waves have been corrected for absorption in final state. The results are shown as directly obtained from and drawn by the computer.
4. Laboratory differential cross section at 10 BeV. Curves (1), (2), (3), and (4) refer to the same steps as on Fig. 3.
5. Laboratory differential cross section at 15 BeV. Curves (1), (2), (3), and (4) refer to the same steps as on Fig. 4.
6. Laboratory differential cross section at 15 BeV. Curves (1), (2), (3), and (4) refer to the same steps as on Fig. 4. The absorption is not assumed to be complete in S-wave but given by (18).
7. K^+ photoproduction via K exchange.

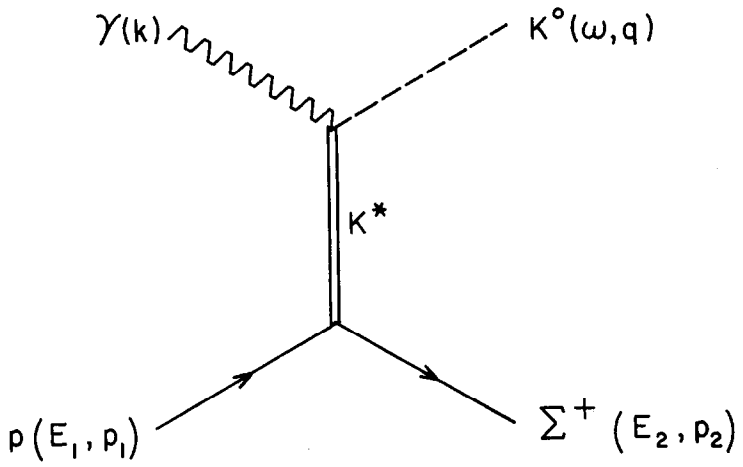

189-1-A

FIG. 1

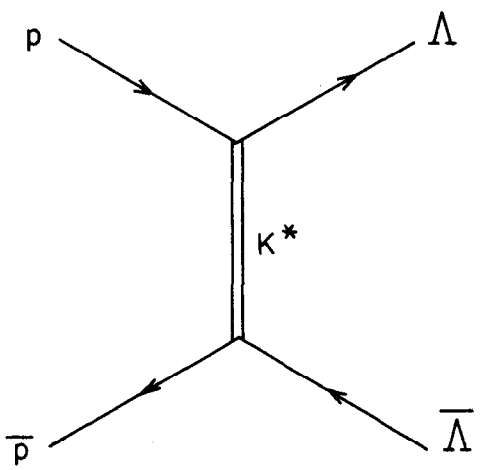

189-2-A

FIG. 2

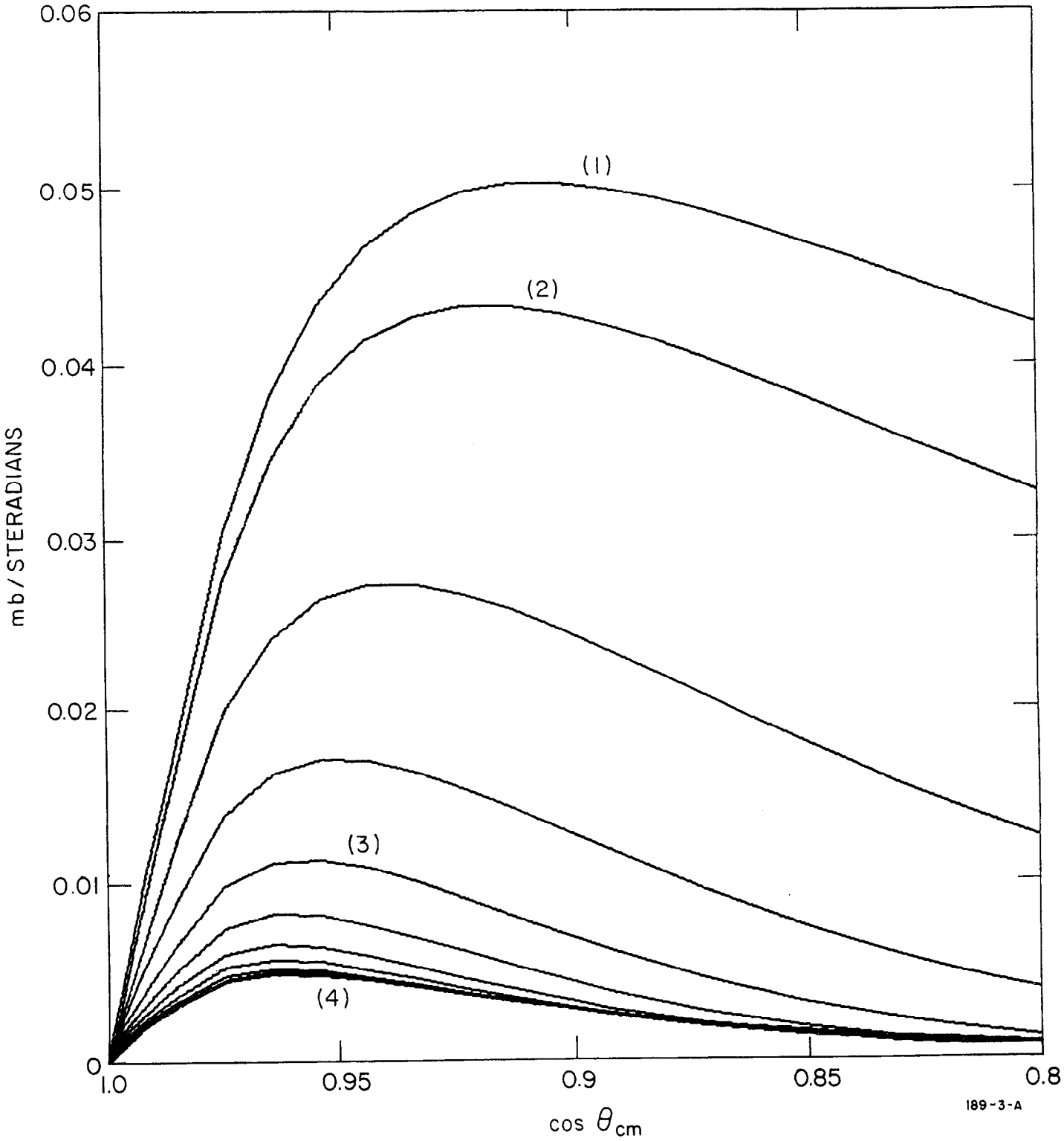
0.06
0.05
0.04
0.03
0.02
0.01
0
mb / STERADIANS
(1)
(2)
(3)
(4)
1.0
0.95
0.9
0.85
0.8
cos θcm
189-3-A

FIG. 3

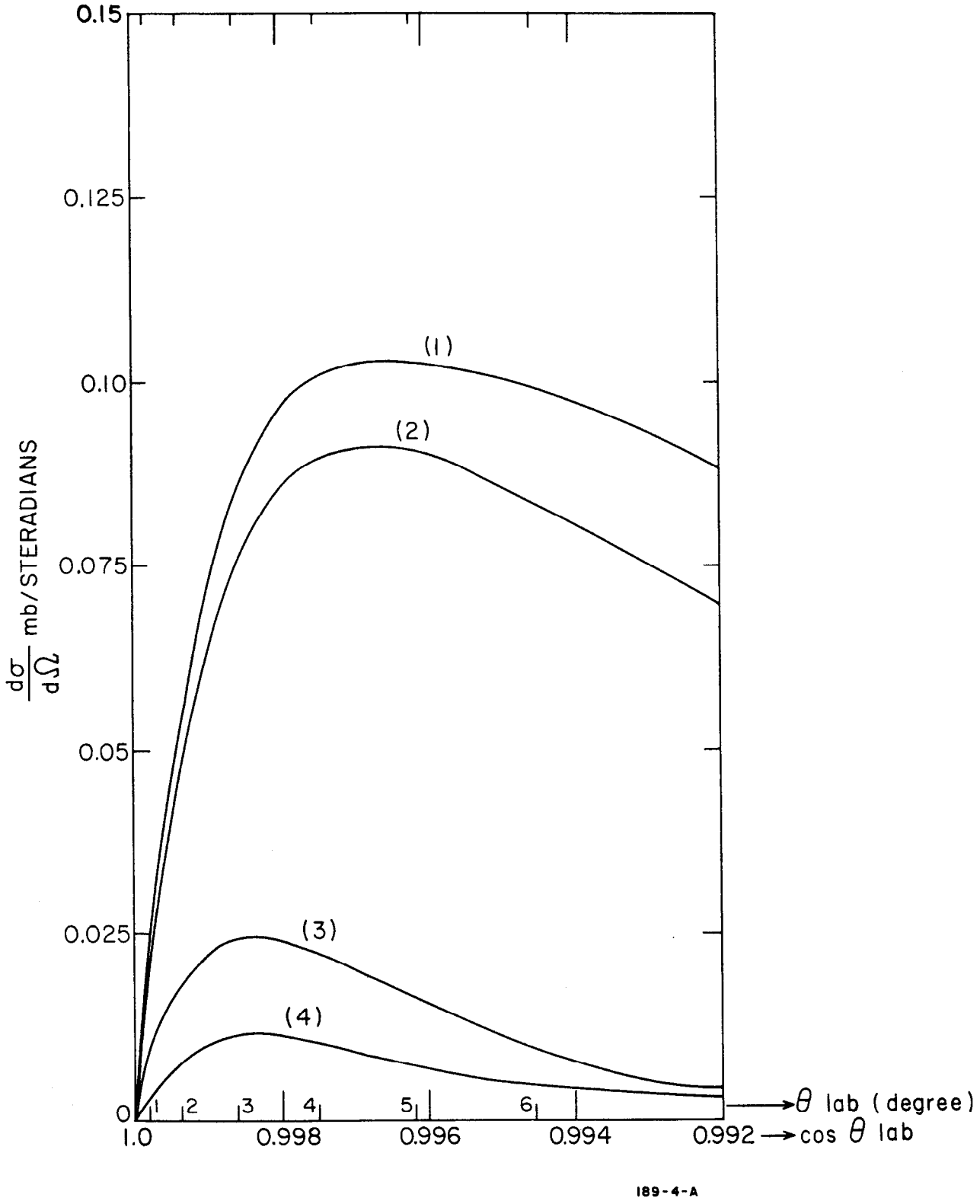
0.15
0.125
0.10
0.075
0.05
0.025
0
(1)
(2)
(3)
(4)
$\frac{d\sigma}{d\Omega}$ mb/STERADIANS
1
2
3
4
5
6
θ lab (degree)
1.0
0.998
0.996
0.994
0.992
cos θ lab
189-4-A

FIG. 4

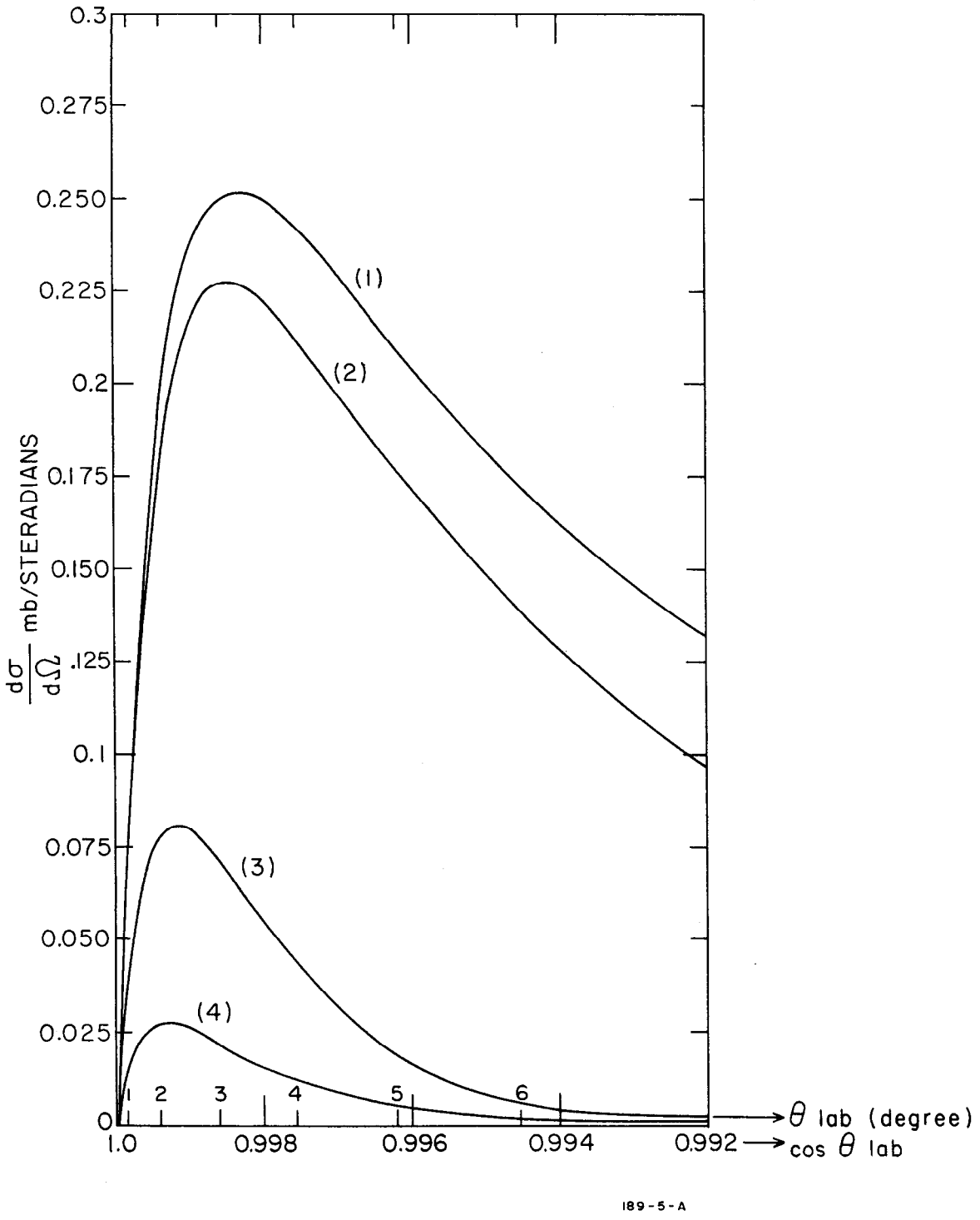
0.3
0.275
0.250
0.225
0.2
0.175
0.150
.125
0.1
0.075
0.050
0.025
0
(1)
(2)
(3)
(4)
1
2
3
4
5
6
1.0
0.998
0.996
0.994
0.992
θ lab (degree)
cos θ lab
dσ/dΩ mb/STERADIANS
189-5-A

FIG. 5

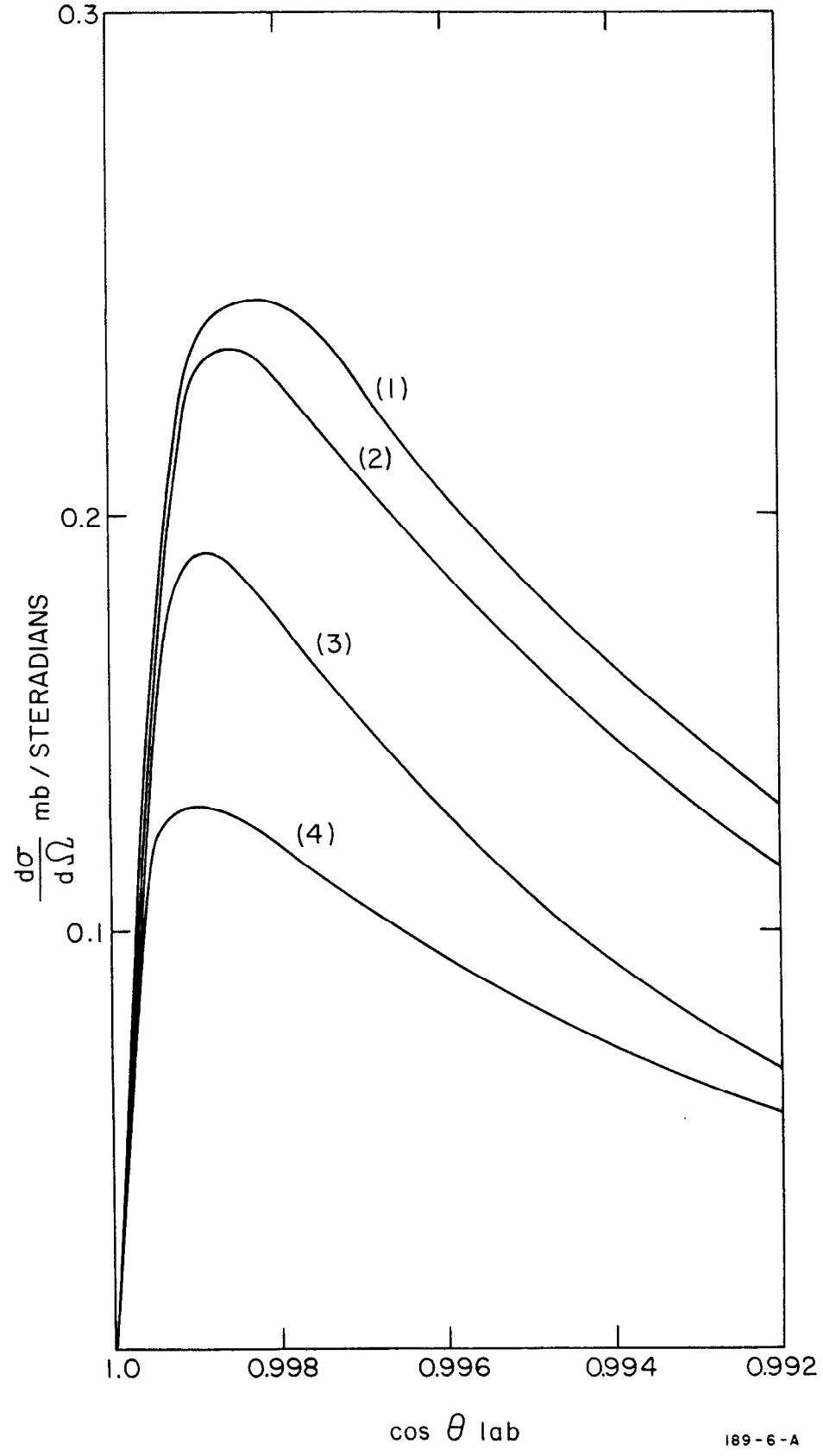
0.3
0.2
0.1
(1)
(2)
(3)
(4)
$\frac{d\sigma}{d\Omega}$ mb / STERADIANS
1.0
0.998
0.996
0.994
0.992
cos θ lab
189-6-A

FIG. 6

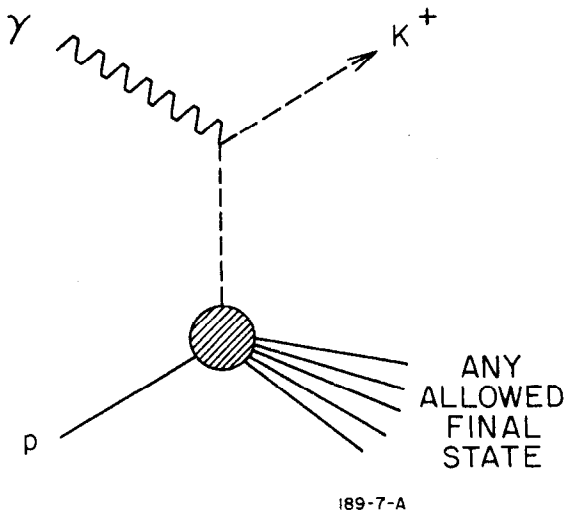

FIG. 7